Liquid Crystals
Publication details, including instructions for authors and subscription information:
http://www.informaworld.com/smpp/title~content=t713926090

A high resolution temperature scanning technique for optical studies of liquid crystal phase transitions

A. Saipa; F. Giesselmann

Online publication date: 11 November 2010

To cite this Article Saipa, A. and Giesselmann, F.(2002) 'A high resolution temperature scanning technique for optical studies of liquid crystal phase transitions', Liquid Crystals, 29: 3, 347 — 353
To link to this Article: DOI: 10.1080/02678290110101912
URL: http://dx.doi.org/10.1080/02678290110101912

LIQUID CRYSTALS, 2002, VOL. 29, NO. 3, 347–353

Taylor & Francis
Taylor & Francis Group

A high resolution temperature scanning technique for optical studies of liquid crystal phase transitions

A. SAIPA and F. GIESSELMANN*

Institute of Physical Chemistry, Clausthal University of Technology, Arnold-Sommerfeld-Str. 4, D-38678 Clausthal-Zellerfeld, Germany

(*Received 26 June 2001; accepted 10 September 2001*)

A temperature scanning attachment for the polarizing microscope is described that offers a simple but powerful technique with which to detect even subtle paramorphotic phase transitions in liquid crystals with high temperature resolution. This technique was applied to CE8, a well known reference compound exhibiting rich mesomorphism. All smectic transitions in CE8 were clearly detected by distinct singularities in the temperature dependence of the transmitted light intensity. Repeated temperature scans across the second order ferroelectric smectic A*–C* transition with various orientations of polarizer and analyser provide high resolution data of optical birefringence and optical tilt angle. These data confirm a mean-field to tricritical crossover in the power law exponent of the optical tilt.

1. Introduction

Since the very beginning of liquid crystal research, phase transitions in liquid crystals have been detected by polarizing microscopy, as these transitions are closely related to distinct changes in birefringence and/or the orientation of the optic axes of the liquid crystal sample. The clearing point and all phase transitions accompanied by changes in the textural topology are easiliy observed in the polarizing microscope. It is more challenging to detect paramorphotic transitions in which the morphology is conserved. For these transitions only subtle changes in the intensity and colour of the transmitted light are observed. An attachment to the microscope of an automated temperature scanning device, containing a computer-controlled hot stage with a temperature sensor, and a photodiode to measure the transmitted light intensity, offers a simple but powerful technique to detect even these subtle paramorphotic transitions by measuring distinct singularities in the temperature dependence of the transmitted light intensity. In the case of well aligned, optically uniform samples, repeated temperature scans at various orientations of polarizer and analyser provide additional information on the birefringence and the optic axis of the liquid crystal sample.

2. Experimental

2.1. *Temperature scanning set-up*

The temperature scanning set-up is schematically shown in figure 1. The sample cell is placed in the computer-controlled hot stage (Instec mK2) of a polarizing microscope (Olympus BH-2). The temperature sensor (PT 100) is placed next to the sample. A photodiode (Photodetector Pin 20, FLC Electronics, Gothenburg) is mounted on the phototube of the microscope to detect the transmitted light intensity. The temperature sensor and photodiode are read out by a data logger (Hewlett Packard 34970A) at certain time intervals, e.g. every second. By continuously heating the sample at a rate of, for example, 0.6 K min^{-1} and sampling the temperature every second, a temperature resolution as high as 10^{-2} K is easily obtained. Temperature gradients, which would smear out singularities at the transition points, are

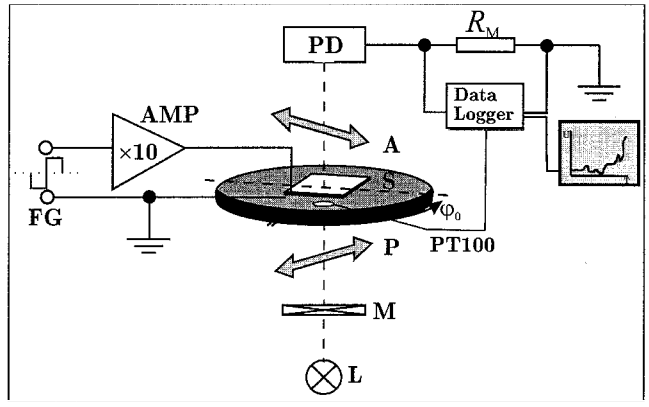

Figure 1. Scheme of the experimental set-up; S = sample, L = light source, M = monochromator (interference filter), P = polarizer, A = analyser, PD = photodiode, FG = function generator, AMP = amplifier, R_M = load resistance, PT100 = temperature sensor.

*Author for correspondence;
e-mail: giesselmann@pc.tu-clausthal.de

Liquid Crystals ISSN 0267-8292 print/ISSN 1366-5855 online © 2002 Taylor & Francis Ltd
http://www.tandf.co.uk/journals
DOI: 10.1080/02678290110101912

avoided by using a high microscope magnification which restricts the measurement to a very small section of the sample, e.g. 400 μm.

Photomicrographs are taken during the scans by a digital camera (Nikon Coolpix 990) replacing one ocular of the binocular microscope. Alignment procedures and electric field dependent measurements are enabled by connecting the cell to a function generator (Hewlett-Packard 8116A) and an amplifier (Krohn Hite model 7500). The light beam can be monochromatized by an interference filter if necessary (see § 3.2).

2.2. *Material and sample preparation*

The temperature scanning technique was applied to the chiral liquid crystal 4-(2-methylbutyl)phenyl 4′-*n*-octylbiphenyl-4-carboxylate, referred to as CE8.

The CE8 sample was placed in a test cell (E.H.C. Co., Ltd., Tokyo) with a cell gap of 4 μm and an active electrode area of 16 mm^2. After filling the cell, non-aligned textures with random orientation of the smectic domains were observed. Well aligned textures were obtained by shear-flow induced by mechanical oscillations of about 100 Hz frequency applied to the upper glass plate of the E.H.C. cell during the N*–A* transition by the vibrator of an electric tooth brush.

3. Results

CE8 is a well known reference compound with rich mesomorphism, exhibiting several smectic phases (F*, I*, C*, A*), crystal phases (G*, J*), a cholesteric phase (N*), and a blue phase [1–4]. Since the phase transitions in CE8 have been disputed for more than 20 years, it is a good selection with which to check the perfomance and reliability of the temperature scanning technique.

3.1. *Phase transition temperatures*

As described in § 2.1 the sample was placed in the hot stage and heated from the crystal G* phase at 40°C to the isotropic phase at about 145°C. During heating at a constant rate of 0.5 K min^{-1}, the temperature T and transmitted light intensity I were read out by the data logger every 3 s leading to a temperature resolution of 0.025 K between adjacent data points. These temperature scans $I(T)$ were recorded for non-aligned and uniformly aligned CE8 samples in polychromatic light, i.e. without the interference filter mentioned in § 2.1. Typical results for aligned and non-aligned samples are shown in figures 3 and 4, respectively. Microphotographs of the liquid crystalline phases, simultaneously taken during the measurements, are also found in these figures.

In general, the liquid crystal phase transitions are reflected by distinct singularities in the $I(T)$ plots. The non-paramorphotic transitions, i.e. the N*–A*, A*–C*, and C*–I* transitions, are easily observed in the aligned and non-aligned samples as discontinuous steps or as abrupt changes in the slope of the $I(T)$ curves; see figures 3(*a*) and 4(*a*), respectively. The singularities observed in the $I(T)$ curve are not related simply to the order of the underlying transition. The second order smectic A*–C* transition is seen as a discontinuous stepwise change of the transmitted light intensity in the aligned sample, figure 3(*a*). In the non-aligned sample the same transition is seen as a discontinuity in the slope of the $I(T)$ curve, figure 4(*b*).

At temperatures below the smectic I* phase a number of transitions between higher ordered smectic and crystal phases are resolved in the expanded temperature scale in figures 3(*b*) (aligned sample) and 4(*b*) (non-aligned sample). The paramorphotic J*–F* and G*–J* transitions are easily seen as stepwise changes in the transmitted light intensity of the aligned sample, figure 3(*b*). The SmI*–SmF* transition is difficult to detect in figure 3(*b*) as the transmission of the aligned sample changes smoothly throughout the transition. This SmI*–SmF* transition is better seen in figure 4(*b*) where the transmission of the non-aligned sample passes a pronounced maximum at the transition point.

From the experimental data in figures 3 and 4, the following phase transition temperatures in °C are obtained with an accuracy at least better than 0.1°C:

Cr 40.0 G* 63.5 J* 66.1 SmF* 67.6 SmI* 69.5
SmC* 86.4 SmA* 137.3 N* 142.0 I

The designation of the higher ordered phases was adopted from the 'LiqCryst' database by Vill [4]. Our phase sequence, i.e. the number of higher ordered phases, confirms the phase sequence found by Kuczyński and Stegemeyer [2], except for the blue phase which was not observed in our thin (4 μm) samples.

In conclusion, the temperature scanning technique clearly leads to the identification of the complex phase sequence of CE8 including all paramorphotic transitions between higher ordered smectic and crystal phases. It is seen from the example of the SmI*–SmF* transition in CE8 that the information obtained from aligned and non-aligned samples is somehow complementary: changes in the transmission of aligned samples are due to changes in the birefringence and changes in the tilt of the optic axes. Since the latter are averaged out in randomly aligned samples, only changes in the birefringence contribute

Figure 2. Structure of CE8.

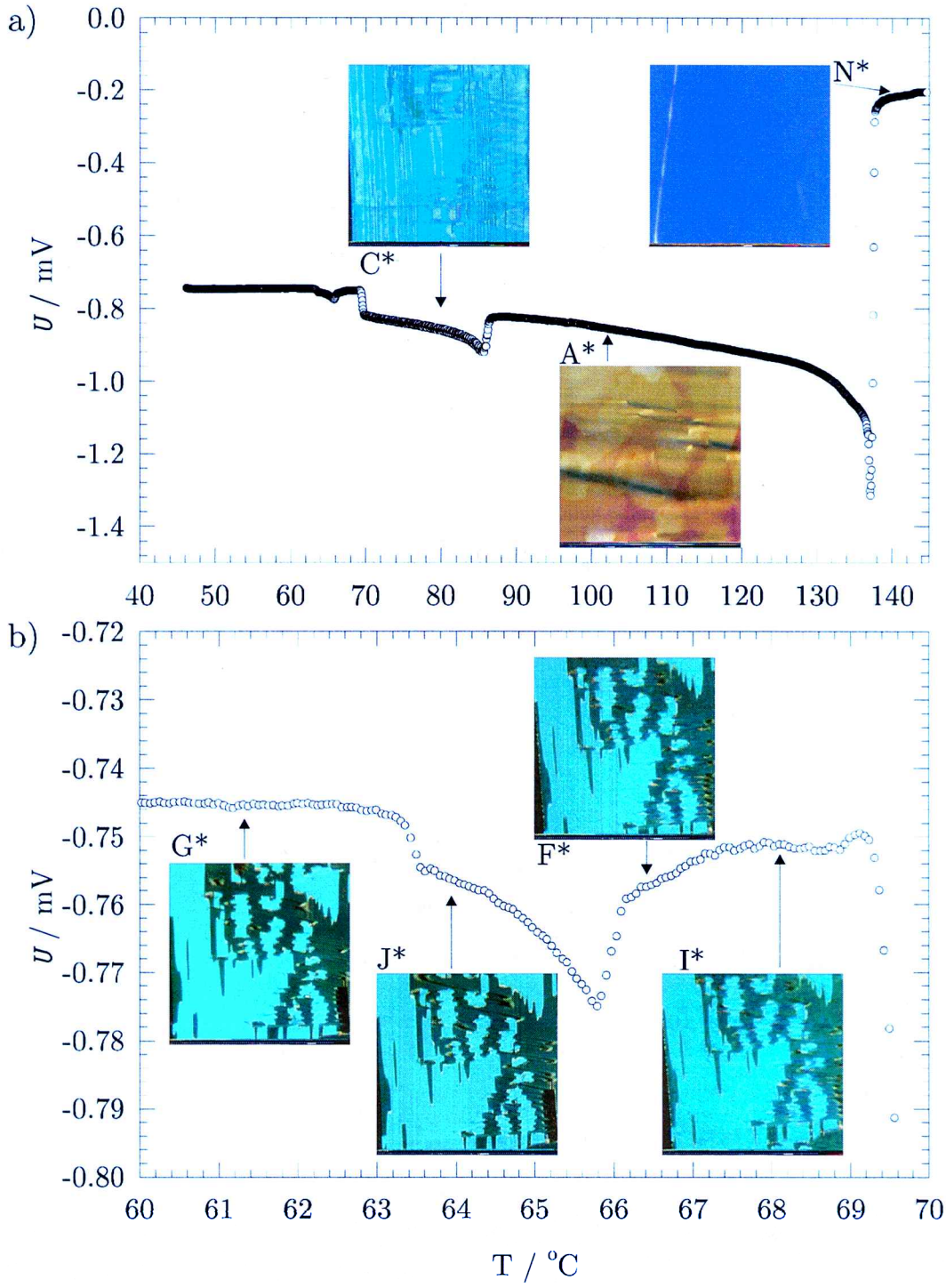

Figure 3. Temperature scan of the aligned CE8 sample: (*a*) complete scan from 40 to 145°C; (*b*) magnification of the higher ordered crystal and smectic phases. *U* denotes the photovoltage measuring the transmitted light intensity *I*.

to the change in transmission of non-aligned samples. The reliability of the temperature scanning technique is considerably improved by the investigation of various sample configurations.

3.2. *Optical tilt angle and birefringence at the SmA*–SmC** *transition*

In a transition from the smectic A to smectic C phases, the director inclines with respect to the smectic

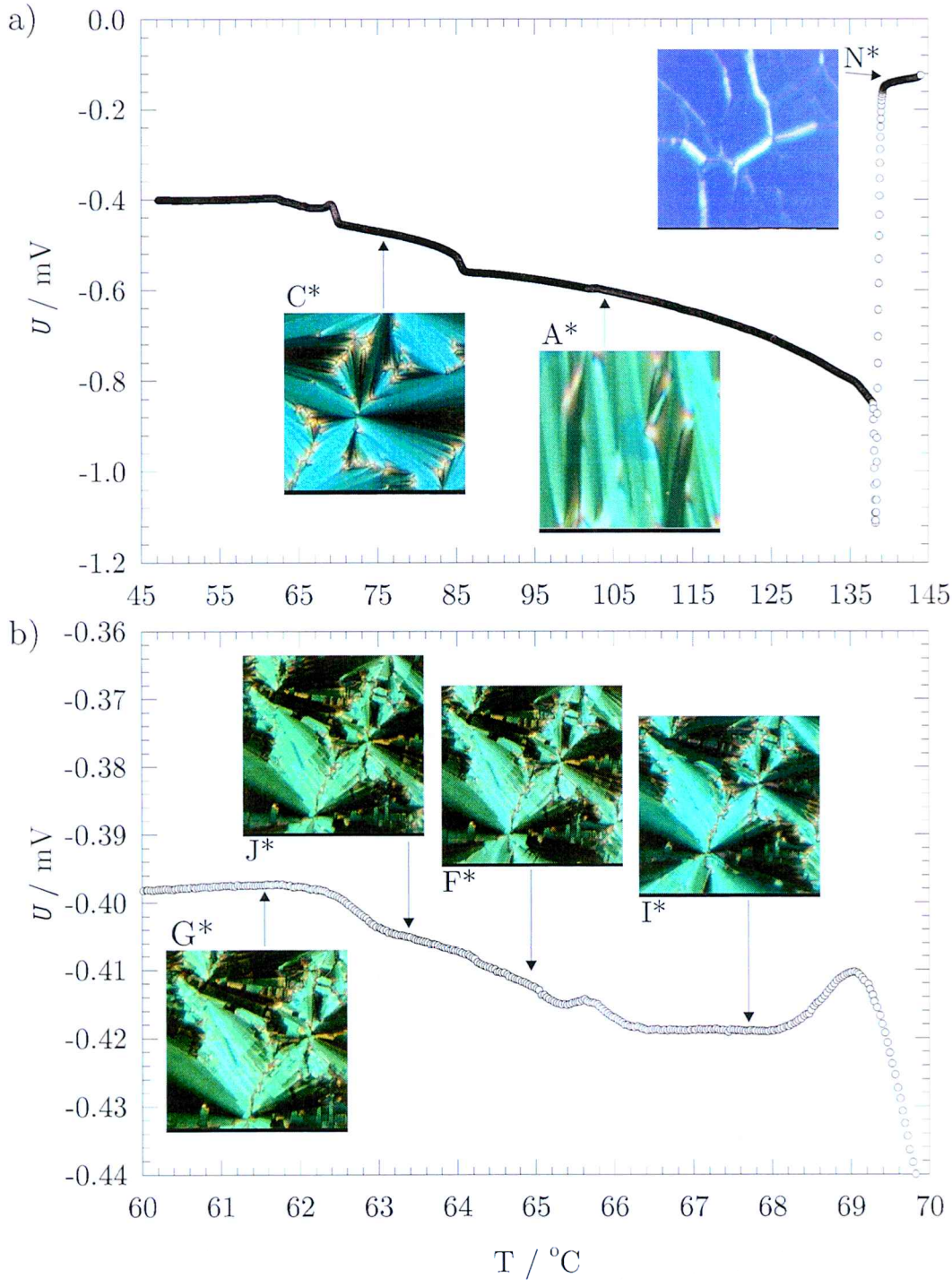

Figure 4. Temperature scan of the non-aligned CE8 sample: (*a*) complete scan from 40 to 145°C; (*b*) magnification of the higher ordered crystal and smectic phases. *U* denotes the photovoltage measuring the transmitted light intensity *I*.

layer normal. The differences in the physical properties between smectic A and smectic C phases are directly related to the director tilt. Hence, the director tilt is considered to be the characteristic order parameter of smectic A–C and chiral smectic A*–C* transitions. It is conveniently measured by the tilt of the optic axis with respect to the layer normal ('optical tilt angle' θ). The temperature scanning technique can be used to measure the optical tilt and the birefringence in a smectic A*–C* transition with high temperature resolution by scanning

the sample transmission at various orientations of the polarizer and analyser.

The liquid crystal is aligned in the so-called 'bookshelf geometry' [5] with the smectic layers perpendicular to the substrates. Under correct surface conditions the SmC director (optic axis) points parallel to the substrates at angles $\pm\theta$ with respect to the smectic layer normal. The sample is considered as a uniaxial birefringent slab with a spatially uniform orientation of the optic axis. At normal incidence of plane-polarized light with wavelength λ and intensity I_0, the transmitted light intensity I of the sample (thickness d, birefringence Δn) between polarizer and analyser is given by [6]:

$$I = I_0\left[\cos^2\chi - \sin 2\varphi \sin 2(\varphi-\chi)\sin^2\frac{\pi d\Delta n}{\lambda}\right] \quad (1)$$

where χ denotes the angle beween polarizer and analyser and φ is the angle between the polarizer and the projection of the optic axis into the substrate plane. Using the general equation (1) four selected situations are considered:

(1) $\varphi=\theta$, $\chi=\pi/2$: The polarizer is directed along the smectic layer normal ($\varphi=\theta$) and the analyser crossed with respect to the polarizer ($\chi=\pi/2$). The resulting light intesity I_1 is given by:

$$I_1 = I_0 \sin^2 2\theta \sin^2\frac{\pi d\Delta n}{\lambda}. \quad (2)$$

(2) $\varphi=\pi/4+\theta$, $\chi=\pi/2$: Polarizer and smectic layer normal include an angle of $\pi/4$ giving $\varphi=\pi/4+\theta$. The light intensity I_2 passing the crossed analyser ($\chi=\pi/2$) is:

$$I_2 = I_0 \cos^2 2\theta \sin^2\frac{\pi d\Delta n}{\lambda}. \quad (3)$$

(3) $\varphi=\theta$, $\chi=0$: Same as case 1 but with parallel polarizers ($\chi=0$) leads to:

$$I_3 = I_0\left(1-\sin^2 2\theta \sin^2\frac{\pi d\Delta n}{\lambda}\right). \quad (4)$$

(4) $\varphi=\pi/4+\theta$, $\chi=0$: Same as case 2 but with parallel polarizers giving:

$$I_4 = I_0\left(1-\cos^2 2\theta \sin^2\frac{\pi d\Delta n}{\lambda}\right). \quad (5)$$

Elimination of the incident light intensity I_0 leads to the transmissions

$$\tau_1 = \frac{I_1}{I_0} = \frac{I_1}{I_1+I_3} = \sin^2 2\theta \sin^2\left(\frac{\pi d\Delta n}{\lambda}\right) \quad (6)$$

$$\tau_2 = \frac{I_2}{I_0} = \frac{I_2}{I_2+I_4} = \cos^2 2\theta \sin^2\left(\frac{\pi d\Delta n}{\lambda}\right) \quad (7)$$

of the cell between crossed polarizers in the orientations discussed above. It is important to mention that both transmissions τ_1 and τ_2 are invariant under a sign inversion of the tilt ($\theta\rightarrow-\theta$). Since opposite tilt directions appear with the same light intensity, equations (6) and (7) also apply to SmC and SmC* samples which, at zero external field, separate into domains of opposite tilt directions. The same holds for a ferroelectric SmC* sample switching between opposite tilt directions in an a.c. electric field.

Considering equations (6) and (7) it is seen that, for given d and λ, any change in the transmission is directly related to changes in the tilt θ and/or the birefringence Δn. These variables are separated as follows. The tilt θ is obtained from the transmission ratio τ_1/τ_2:

$$\frac{\tau_1}{\tau_2} = \tan^2(2\theta) \quad (8)$$

to be:

$$\theta = \frac{1}{2}\arctan\left(\frac{\tau_1}{\tau_2}\right)^{1/2}. \quad (9)$$

The birefringence Δn is calculated from the sum $\tau_1+\tau_2$:

$$\tau_1+\tau_2 = \sin^2\left(\frac{\pi d\Delta n}{\lambda}\right) \quad (10)$$

as:

$$\Delta n = \frac{\lambda}{\pi d}\arcsin(\tau_1+\tau_2)^{1/2}. \quad (11)$$

This approach has been applied to CE8 as follows. As the evaluation of equations (6) and (7) requires a defined wavelength, an interference filter with $\lambda=514$ nm was inserted into the set-up (see § 2.1). Repeated temperature scans were taken during heating the well aligned CE8 sample from 80 to 90°C in the four different orientations discussed above. The corresponding light intensities $I_1,\ldots,I_4$ are depicted in figure 5. From the intensity data in figure 5 the optical tilt θ and the birefringence Δn are calculated using equations (9) and (11), respectively. The results are shown in figure 6.

Below the smectic A*–C* transition at $T_{CA}=86.4$°C the optical tilt is continuously increasing, clearly reflecting the second-order smectic A*–C* transition in CE8, see figure 6(*a*). Well below the transition at $T-T_{CA}=-6$°C the tilt is about 10°, a comparatively small value which was also observed in other experiments [7]. The birefringence remains basically unchanged during the A*–C* transition see figure 6(*b*). The drop observed directly at the transition temperature is most probably an artefact due to critical fluctuations lowering the transmission of the sample by light scattering, which is not included in equations (6) and (7). From the width

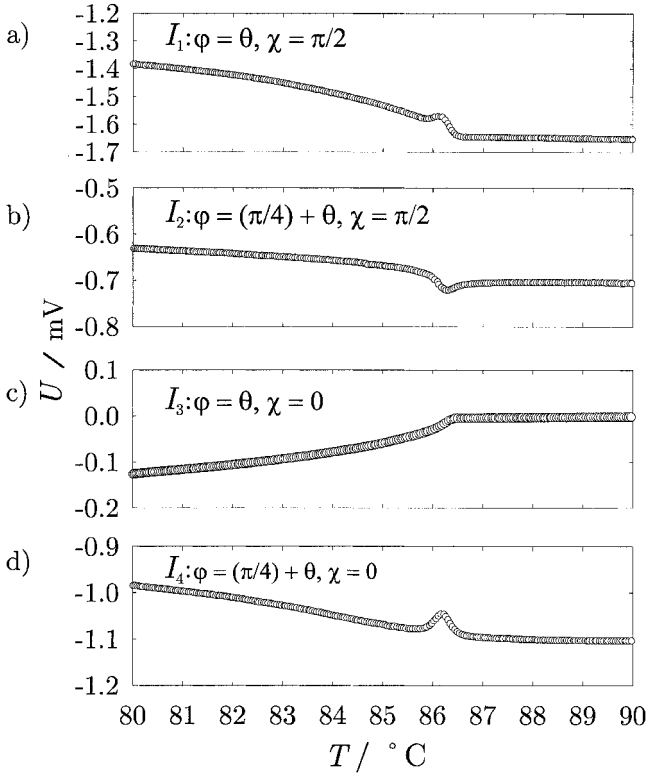

Figure 5. Photovoltage U measuring the transmitted light intensity obtained in repeated temperature scans at four different orientations χ, φ of polarizer and analyser. For explanations see text.

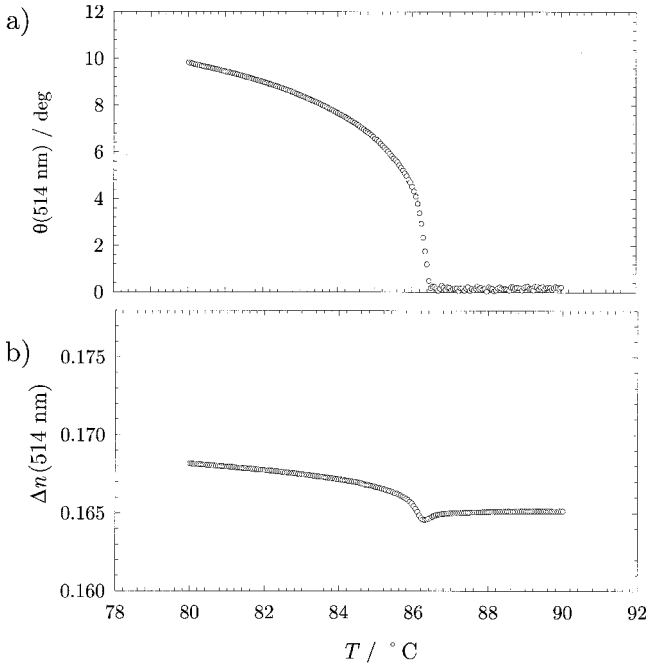

Figure 6. (*a*) Optical tilt angle θ and (*b*) birefringence Δn of CE8 at optical wavelength $\lambda = 514$ nm.

of the scattering peak in figure 6(*b*) the critical regime is estimated to about 0.4 K in the case of the CE8 smectic A*–C* transition.

The tilt angle exponent β which is the critical exponent of the smectic A*–C* order parameter in the case of $T \rightarrow T_{CA}$ is obtained from the power law:

$$\theta \propto (T_{CA} - T)^{\beta} \tag{12}$$

with $T \leqslant T_{CA}$. The log–log plot of the temperature dependence of the optical tilt angle is shown in figure 7 and a clear power law behaviour is observed. Close to the transition to smectic A* in the range of $T_{CA} - T = 0.04 \ldots 0.25$ K the classical mean-field exponent $\beta = 0.53 \approx 1/2$ is found. At about $T_{CA} - T = 0.3$ K the crossover to the tricritical exponent $\beta = 0.32 \approx 1/3$ is observed. These results agree with the results of Muševič *et al.* [7] who found a crossover from $\beta = 0.49$ to $\beta = 0.35$. The crossover temperature (86.1°C) comes close to the onset of critical fluctuations which are observed by the drop in birefringence $\Delta n(T)$ between about 86.1 and 86.5°C in figure 6(*b*).

4. Conclusions

The results obtained from CE8 clearly lead to the conclusion that the proposed scanning technique offers a simple but powerful tool in the optical investigation of liquid crystal phase transitions, specifically:

(1) Even in the case of rather complex mesomorphism, liquid crystal phase transitions are clearly detected by singularities in the temperature dependence of the sample transmission between crossed polarizers. In CE8 all transitions between six smectic and crystal phases were detected and the phase sequence

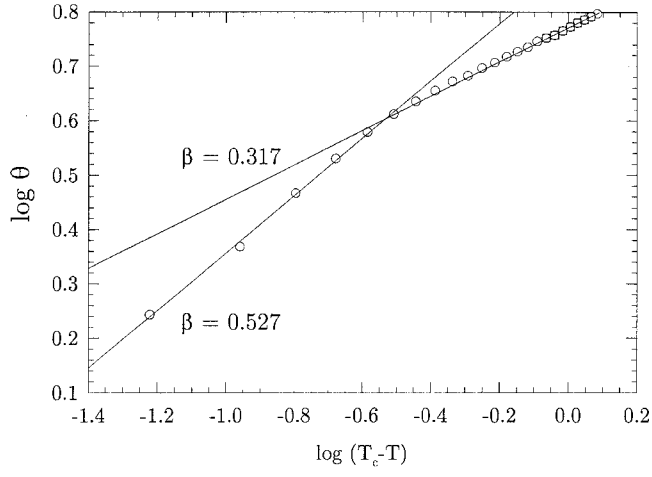

Figure 7. Determination of the order parameter exponent β in the smectic C* phase of CE8. Close to the transition the classical mean-field exponent $\beta \approx 1/2$ is found.

found by Kuczyński and Stegemeyer [2] was confirmed.

(2) In well aligned samples high resolution data of the optical tilt angle and the effective birefringence are accessible by repeated temperature scans at various orientations of polarizer and analyser.

(3) The resolution of the obtained tilt data allows a reliable determination of power-law exponents and, in the case of CE8, confirms the mean-field to tricritical crossover found by Muševič *et al.* [7].

Financial support from the *Fonds der Chemischen Industrie* is gratefully acknowledged.

References

[1] Goodby, J. W., and Gray, G. W., 1979, *J. Phys. Coll.*, **40,** C3-27.

[2] Kuczyński, W., and Stegemeyer, H., 1989, *Liq. Cryst.*, **5,** 553.

[3] Dierking, I., Andersson, G., Komitov, L., Lagerwall, S. T., and Stebler, B., 1997, *Ferroelectrics*, **193,** 1.

[4] http://liqcryst.chemie.uni-hamburg.de/lolas-www/main.html

[5] Clark, N. A., and Lagerwall, S. T., 1980, *Appl. Phys. Lett.*, **36,** 899.

[6] Born, M., 1972, *Optik* (Berlin: Springer-Verlag).

[7] Muševič, I., Škarabot, M., Kityk, A. V., Blinc, R., Moro, D., and Heppke, G., 1997, *Ferroelectrics*, **203,** 133.